Mobile Sensor Network Control Using Mutual Information Methods and Particle Filters

Gabriel M. Hoffmann, *Member, IEEE*, and Claire J. Tomlin, *Senior Member, IEEE*

***Abstract*—This paper develops a set of methods enabling an information-theoretic distributed control architecture to facilitate search by a mobile sensor network. Given a particular configuration of sensors, this technique exploits the structure of the probability distributions of the target state and of the sensor measurements to control the mobile sensors such that future observations minimize the expected future uncertainty of the target state. The mutual information between the sensors and the target state is computed using a particle filter representation of the posterior probability distribution, making it possible to directly use nonlinear and non-Gaussian target state and sensor models. To make the approach scalable to increasing network sizes, single-node and pairwise-node approximations to the mutual information are derived for general probability density models, with analytically bounded error. The pairwise-node approximation is proven to be a more accurate objective function than the single-node approximation. The mobile sensors are cooperatively controlled using a distributed optimization, yielding coordinated motion of the network. These methods are explored for various sensing modalities, including bearings-only sensing, range-only sensing, and magnetic field sensing, all with potential for search and rescue applications. For each sensing modality, the behavior of this non-parametric method is compared and contrasted with the results of linearized methods, and simulations are performed of a target search using the dynamics of actual vehicles. Monte Carlo results demonstrate that as network size increases, the sensors more quickly localize the target, and the pairwise-node approximation provides superior performance to the single-node approximation. The proposed methods are shown to produce similar results to linearized methods in particular scenarios, yet they capture effects in more general scenarios that are not possible with linearized methods.**

***Index Terms*—Active sensing, cooperative systems, distributed control, entropy, intelligent sensors, mobile sensor network, Monte Carlo methods, mutual information, particle filter.**

I. Introduction

MOBILE sensor networks can be deployed to efficiently acquire information about the world, such as the location of a search target, with the ability to make simultaneous measurements from multiple vantage points. The control objective is to search for information quickly, safely, and reliably. Limitations in sensor capabilities can render this a challenging task. This paper develops methods to automate mobile sensors to meet this control objective using a probabilistic, non-heuristic foundation. Given a set of sensors, these techniques exploit the structure of the probability distributions of the target state and of the sensor measurements to compute control inputs leading to future observations that minimize the expected future uncertainty of the target state.

Several computational challenges arise in searching for a target. First, there is the task of representing information. Typically, there is low prior information available about the target's state. Search regions can be complicated to represent. As the search progresses, the target state probability distribution often requires a more intricate model than can be represented by a parametric distribution, such as Gaussian. Further, the mapping between sensor observations and the physical world, even for simple sensors, is frequently a nonlinear function, such as the $\arctan$ function for bearing measurements, and the $\mathcal{L}^2$ norm for range measurements, neither of which is one-to-one. Second, there is the challenge of formulating the optimal control problem. The linear, quadratic cost, Gaussian distribution (LQG) assumptions that lead to the certainty equivalence principle, separating the estimation and control problems, are typically not valid in this problem [1]. Third, there is the difficulty of cooperatively controlling the mobile sensors. In order to improve network performance, it would be desirable to add more sensors to the network while keeping the computational cost of optimizing the actions bounded. Also, safety requirements must be satisfied, such as collision avoidance between vehicles. They must maintain a safe separation distance under the constraints of their dynamics.

We propose two techniques to address these challenges, in order to yield a mobile sensor network framework which is scalable and capable of accurately capturing and using information. The first technique is to directly use particle filter estimators [2] to compute an information seeking objective function. This enables the use of multi-modal posterior distributions, nonlinear and non-Gaussian sensor models, and the use of general prior information. This technique preserves details in the objective function that would be discarded by linearization and Gaussian approximations—it is possible to more accurately quantify the value of potential observations. The second technique is to decompose the information seeking objective function so that as the number of vehicles increase, the vehicles can leverage one another's positions to improve the sensing capabilities using approximations that discard higher order terms. A first approximation is to fully decouple the problem. We define

Manuscript received November 01, 2007; revised November 20, 2008. First published December 08, 2009; current version published January 13, 2010. This work was supported by ONR under the CoMotion MURI Contract N00014-02-1-0720, and in part by AFOSR under the Multi-University Research Initiative (MURI) Grant FA9550-06-0312. Recommended by Associate Editor K. H. Johansson.

G. M. Hoffmann is with the Intelligent Systems Lab, Palo Alto Research Center (PARC), Palo Alto, CA 94304 USA (e-mail: gabeh@parc.com).

C. J. Tomlin is with the Department of Electrical Engineering and Computer Sciences, University of California, Berkeley, CA 94720USA. She is also with the Department of Aeronautics and Astronautics, Stanford University, Stanford, CA 94305 USA (e-mail: tomlin@eecs.berkeley.edu).

Color versions of one or more of the figures in this paper are available online at http://ieeexplore.ieee.org.

Digital Object Identifier 10.1109/TAC.2009.2034206

this as the *single-node* approximation, and derive the error incurred. Its computational complexity is constant with respect to the number of sensors, yielding a fast distributed cooperative optimization. Although the vehicles appear to cooperate due to optimization using the same target state probability distribution, the only interactions between their local optimization problems are the collision avoidance constraints. To enable a higher level of cooperative sensing, we propose a new method that considers the effects of each sensor on each other sensor, pairwise, the *pairwise-node* approximation. It incurs a linear computational expense in the number of vehicles, yet the effect of the approximation error is provably reduced from that of the single-node approximation, allowing coupled effects between mobile sensors to be captured.

To evaluate the characteristics of the proposed algorithms, we explore three sensing modalities. The first is bearings-only sensing, such as cameras and directional antennae [3], where the direction to the target is measured. This permits comparison to related work. The second is range-only sensing, including techniques such as received signal strength measurements and time-of-flight measurements [4], in which distance to the target is measured. Localization using this modality is more prone to error using standard linearization techniques, but control actions generated using the non-parametric algorithms presented here match the analytically optimal behavior. The final modality is personal radio beacons, such as those used for avalanche rescue [5]. Here, the dipole magnetic field emitted by the beacon is measured, with a nonlinear periodic shape—the posterior probability distribution of the state estimate can be substantially non-Gaussian. In all scenarios, the mobile sensor dynamics are modeled to be the dynamics of the quadrotor helicopters in the Stanford Testbed of Autonomous Rotorcraft for Multi-Agent Control (STARMAC) [6].

This search problem is a stochastic optimal control problem—control inputs regulate both the dynamics of the system and the information gained by sensing, as discussed in work on the dual control problem [7] and on extremum-seeking control [8]. Several stochastic optimal control problems have been solved by simplifying sensor and motion models, such as the LQG problem [1]. The assumptions of the LQG problem were extended to target localization using the Extended Kalman Filter (EKF), which linearizes motion and measurement models. These methods use metrics of the expected estimation covariance, often in an information theoretic context [9]–[12]. A feedback controller was formulated for dual control using an EKF with assumptions rendering the solution suboptimal, but solvable online [13].

Although EKF approaches are computationally efficient, they use linearized measurement models, rely on a Gaussian noise assumption, and require a guessed initial solution. This can lead to underestimation of the covariance, biased estimates, and divergence of the filter [2], [14]–[16]. These drawbacks can be mitigated through a number of methods, but they cannot be eliminated [15], [17]. The EKF methods also approximate the structure of posterior distributions with only a mean and a covariance, discarding additional available information. One method to improve on EKF performance uses grid cell discretization for estimation, though it uses a probability-of-detection model for the sensor rather than a complete sensor model [18]. The work presented in this paper also uses metrics of the underlying estimator, although by using a particle filter as the estimator, the nonlinear estimation performance can be improved, more information can be captured, and explicit sensor models can be incorporated.

Information theoretic costs metrics have been used to manage sensors [19], and led to algorithms to control sensor networks for information gathering over an area by parameterizing the motion of collectives of vehicles [20]. The optimal probing control law to minimize Shannon entropy for the dual control problem was shown to be the input that maximizes mutual information [21]. A property relating probability distributions, the alpha-divergence, was computed for particle filters and applied to manage sensors with binary measurements, though scalability in sensor network size was not addressed, and Shannon entropy was only found in the limit of the presented equations [22]. Probability-of-detection was computed using both grid cell and particle filter estimators, and experimentally demonstrated [23]. An approximate method was used to estimate the expected entropy for particle filters over a finite horizon [24]. Gaussian particle filtering was used with a mutual information objective function, though the technique approximates the posterior probability distribution as Gaussian at every update [25]. An earlier version of mutual information approximation techniques was presented in [26]. The work presented here develops methods to make the information theoretic ideas of previous work tractable and scalable for real-time control of a mobile sensor network for general sensors, dynamics, and available prior knowledge.

The theoretical contributions of this paper are three-fold. First, formulae are derived to compute information theoretic quantities for a particle filter representation of probability distributions. Second, single-node and pairwise-node approximations are derived for the mutual information available in a mobile sensor network, with general probability density models, analytical bounds on the error incurred, and computation time that is polynomial in the number of sensors. Third, the pairwise-node approximation is proven to be a more accurate objective function for mutual information optimization than the single-node approximation. The benefits of these contributions are explored for three different sensing modalities.

We proceed in Section II by formulating the problem and showing the equivalence of searching for a target and maximizing mutual information. Then, algorithms are derived to compute mutual information using particle filters in Section III, and used in a distributed control algorithm to cooperatively control the vehicles. The methods are applied in simulation in Section IV to the three sensing modalities described above. The results in these examples show successful localization under all tested circumstances, due to the underlying particle filter. The pairwise-node approximation leads to faster localization than using the single-node approximation, and increasing the size of the network speeds localization. Successful localization of the rescue beacon's magnetic field source exemplifies the utility of these techniques.

II. Problem Formulation

This section defines the search problem and proposes an information-theoretic framework for the solution. First, the mobile sensor network model is defined, then the goal of searching for a target is cast using the information-theoretic concept of mutual information as a utility function to optimally search for a target.

A. Mobile Sensor Motion and Measurement Models

Consider a set of n_v vehicles carrying sensors to locate a target in the search domain $\boldsymbol{\Theta}$. The state of the target $\boldsymbol{\theta}_t \in \boldsymbol{\Theta} \subset \mathbb{R}^{n_\theta}$ at discrete time t is unknown to the vehicles. Though we consider stationary targets here, a motion model could be used for nonstationary targets [27]. A prior distribution $p(\boldsymbol{\theta}_0)$ is provided, using any information available *a priori*.

The state of the i^{th} vehicle is $\mathbf{x}_t^{(i)} \in \mathbb{R}^{n_s}$, with n_s vehicle states, such as position, orientation, and velocity. The discrete time dynamics are

$$\mathbf{x}_{t+1}^{(i)} = f_t^{(i)}(\mathbf{x}_t^{(i)}, \mathbf{u}_t^{(i)}) \tag{1}$$

where $\mathbf{u}_t^{(i)} \in U^{(i)} \subset \mathbb{R}^{n_u}$ is the set of n_u control inputs, $U^{(i)}$ is their domain, and the time duration between time steps is Δ. The collision avoidance constraint imposed between vehicles is a minimum separation of $\bar{d}$. This accounts for the finite expanse of the vehicles and safety margin. Let $\boldsymbol{\rho}_t^{(i)}$ be the subset of the i^{th} vehicle's states that corresponds to its position. The collision avoidance constraint is

$$\|\boldsymbol{\rho}_t^{(i)} - \boldsymbol{\rho}_t^{(j)}\| \geq \bar{d} \qquad \forall j \in \{1, \ldots, n_v : j \neq i\}. \tag{2}$$

Sensor measurements for the i^{th} vehicle $\mathbf{z}_t^{(i)} \in Z^{(i)} \subset \mathbb{R}^{n_z}$ are taken at rate $1/\Delta$, where $Z^{(i)}$ is the domain of the observations, with dimension n_z. When the superscript is omitted, $\mathbf{z}_t = \{\mathbf{z}_t^{(1)}, \ldots, \mathbf{z}_t^{(n_v)}\}$. The measurement model is

$$\mathbf{z}_t^{(i)} = h_t^{(i)}(\mathbf{x}_t^{(i)}, \boldsymbol{\theta}, \boldsymbol{\eta}_t^{(i)}). \tag{3}$$

Observation noise $\boldsymbol{\eta}_t^{(i)} \in \mathbb{R}^{n_\eta}$ has an assumed probability distribution $p(\boldsymbol{\eta}_t^{(i)})$ which need not be Gaussian. The problem formulation admits a broad class of measurement models, as $h_t^{(i)}$ could be a nonlinear or discontinuous mapping of the states and measurement noise onto the observation space. Each vehicle is provided the measurement model for all sensors in the network *a priori*. This enables each vehicle to interpret observations made by any sensor in the network and model their capabilities, making possible optimal trajectory planning as described in the following section. Note that the measurement model for a sensor must be known in order to use it, so sharing the measurement models between vehicles introduces no practical limitations in this cooperative scenario.

For computational purposes, each vehicle must store the posterior distribution locally. To enable distributed knowledge of this distribution, using non-parametric estimators, each vehicle i maintains its own instantiation of the posterior distribution of the target state $p(\boldsymbol{\theta}_t)$ incorporating all prior measurements, $\{\mathbf{z}_1, \ldots, \mathbf{z}_{t-1}\}$. The local instantiation of $p(\boldsymbol{\theta}_t)$ is a non-parametric approximation to the true posterior distribution. The system is assumed to be Markov, hence recursive updates using Bayes' rule are used to incorporate observations made or received between time $t-1$ and t,

$$p(\boldsymbol{\theta}_t|\mathbf{z}_t) = \frac{p(\boldsymbol{\theta}_t)p(\mathbf{z}_t|\boldsymbol{\theta}_t)}{p(\mathbf{z}_t)}. \tag{4}$$

The target is assumed stationary for this work, so recursion is accomplished using $p(\boldsymbol{\theta}_t) = p(\boldsymbol{\theta}_{t-1}|\mathbf{z}_{t-1})$. To incorporate a nonstationary target, a motion model would provide this relationship. All vehicles' distributions are based on the full history of shared observations, and can be assumed nearly identical. It is assumed that the vehicles are equipped with communication devices that enable this exchange of measurements between vehicles. One such reliable technology is demonstrated in the 802.11g network used for STARMAC [6]. Although the methods presented are tolerant of imperfect communication in practice, the implications of communication quality on the control objective is a current area of research.

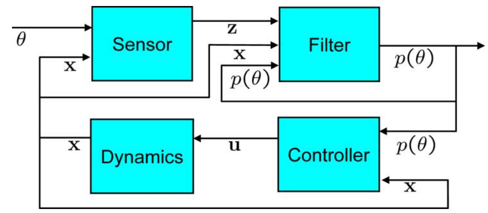

Fig. 1. As in a standard control system, the state vectors $\mathbf{x}$ of the vehicles are manipulated using the control inputs $\mathbf{u}$. Unlike a typical control system, the information-seeking controller receives the full probability distribution $p(\boldsymbol{\theta})$ of the target state estimate vector $\boldsymbol{\theta}$, rather than only the expected value. The future value of $\mathbf{x}$ can be controlled such that future sensor measurements $\mathbf{z}$ yield the greatest expected reduction in the uncertainty of $p(\boldsymbol{\theta})$, based on sensors models. The vehicles maximize the information gained about the target state while minimizing the number of future measurements required.

B. Information Seeking

The goal of the search team differs from a typical control system. The measurement of success is not the ability to track a trajectory—rather, as depicted in Fig. 1, it is to maximize the likelihood of localizing the target as quickly as possible. The target is localized by making observations at a fixed rate. The more observations required, the slower the target is localized. Therefore, the goal can equivalently be stated as *controlling sensor locations* to *minimize the expected number of future observations needed to ascertain the target's state*. A set of observations can be interpreted, in an information-theoretic sense, as a code word, with an alphabet comprised of all possible quantized outputs of the n_z sensors. These encode the target state, which is represented numerically in software by a finite alphabet of symbols, such as 64 bits in a double precision floating point data type. Therefore, to minimize the expected number of remaining observations is to maximize the expected log-likelihood of the posterior distribution with each observation of the vehicles, as derived in [28].

In order to increase this likelihood as quickly as possible at each time step, only the control actions for the current time step need be considered. To optimize control actions over longer time horizons, it is equivalent to using a larger code word, in information theoretic terms. Although a longer optimization horizon results in equal or better expected performance by the end of the time horizon, the one step horizon maximizes the *current* rate at which information is acquired, yielding equal or better expected results by the next time step. Interesting bounds on the tradeoff are given by [25]. To satisfy the goal of acquiring information as quickly as possible for the time-critical search problem—with diminishing returns for delayed information—one step horizons are considered here.

Taking the log-likelihood of the posterior distribution given by Bayes' rule in (4), and using $p(\mathbf{z}_t, \boldsymbol{\theta}_t) = p(\mathbf{z}_t|\boldsymbol{\theta}_t)p(\boldsymbol{\theta}_t)$ yields

$$H(\boldsymbol{\theta}_t|\mathbf{z}_t) = H(\boldsymbol{\theta}_t) - I(\mathbf{z}_t;\boldsymbol{\theta}_t) \tag{5}$$

where

$$H(\boldsymbol{\theta}_t) = -\int_{\boldsymbol{\theta}\in\boldsymbol{\Theta}} p(\boldsymbol{\theta}_t)\log p(\boldsymbol{\theta}_t)d\boldsymbol{\theta}, \tag{6}$$

$$H(\boldsymbol{\theta}_t|\mathbf{z}_t) = -\int_{\substack{\boldsymbol{\theta}\in\boldsymbol{\Theta}\\ \mathbf{z}\in Z}} p(\boldsymbol{\theta}_t,\mathbf{z}_t)\log p(\boldsymbol{\theta}_t|\mathbf{z}_t)d\boldsymbol{\theta}d\mathbf{z}, \tag{7}$$

$$I(\mathbf{z}_t;\boldsymbol{\theta}_t) = \int_{\substack{\boldsymbol{\theta}\in\boldsymbol{\Theta}\\ \mathbf{z}\in Z}} p(\boldsymbol{\theta}_t,\mathbf{z}_t)\log\frac{p(\boldsymbol{\theta}_t,\mathbf{z}_t)}{p(\boldsymbol{\theta}_t)p(\mathbf{z}_t)}d\boldsymbol{\theta}d\mathbf{z}. \tag{8}$$

$H(\boldsymbol{\theta}_t)$ is the *entropy* of the target state distribution, $I(\mathbf{z}_t;\boldsymbol{\theta}_t)$ is the *mutual information* between the distributions of the target state and the sensors, and $H(\boldsymbol{\theta}_t|\mathbf{z}_t)$ is the *conditional entropy*[1] of the distribution—the expected entropy of the target state when conditioning with $\mathbf{z}_t$[29]. The entropy of a probability distribution is a metric of its uncertainty. The mutual information is a metric of the expected divergence (Kullback-Liebler) between the independent and joint distributions of $\boldsymbol{\theta}_t$ and $\mathbf{z}_t$. It is large when two distributions have strong interdependence, and zero when they are independent.

Control inputs $\mathbf{u}_t$ and vehicle states $\mathbf{x}_t$ influence observations $\mathbf{z}_t$ through (1) and (3). To minimize the expected future uncertainty of the target state distribution with respect to $\mathbf{u}_t$ is to minimize (5). Note that the actual uncertainty can only be determined once the true measurement $\mathbf{z}_t$ is made. The prior uncertainty is independent of the future control inputs, as depicted in Fig. 2, so to minimize the expected posterior uncertainty, one must maximize the observation information with respect to the control inputs.

In order to seek information, the network computes its control inputs by maximizing the mutual information utility function, defined as follows

Definition 1 (Mutual Information Utility Function): The mutual information utility function evaluated at vehicle i is

$$V^{(i)}(\mathbf{x}_t, \mathbf{u}_t, p(\boldsymbol{\theta}_t)) = I(\mathbf{z}_{t+1};\boldsymbol{\theta}_{t+1}) \tag{9}$$

where argument $p(\boldsymbol{\theta}_t)$ indicates that the data defining the probability distribution of $\boldsymbol{\theta}_t$ are used by the utility function. The arguments on the right hand side of (9) are random variables; to evaluate this expression requires the sensor model, (3), and vehicle motion model, (1). Both are functions of the arguments of the mutual information utility function.

Methods for computing this utility function are presented in the next section.

[1]When the argument of $H(\cdot)$ indicates a conditional relationship, e.g., $a|b$, it is the expected entropy of the conditional probability distribution $p(a|b)$, since b is a random variable. Thus, $H(a|b) = \int_{b\in\mathcal{B}} p(b)\left(\int_{a\in\mathcal{A}} p(a|b)\log p(a|b)da\right)db$. Because $p(a,b) = p(a|b)p(b)$, this is equal to the expression in (7). If the value of b were known to be a constant b_c, then the entropy would be $H(a|b = b_c)$, which can be computed without taking an expectation.

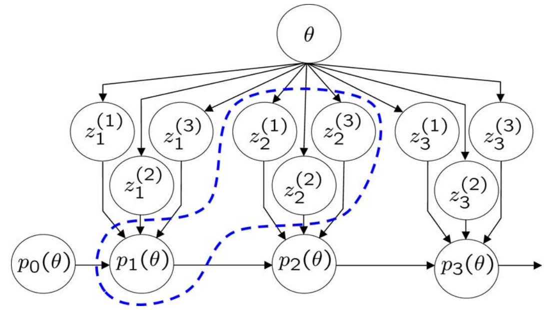

Fig. 2. Directed graphical model of the estimator with 3 mobile sensors. The dashed line region contains the random variables used in the information theoretic optimization to compute the control actions at time $t = 1$. The optimization finds control actions that minimize the expected uncertainty of the subsequent target state model $p_2(\boldsymbol{\theta})$, a function of the probability distributions of the random variables $\mathbf{z}_2^{(1)}$, $\mathbf{z}_2^{(2)}$, and $\mathbf{z}_2^{(3)}$, and the current target state model $p_1(\boldsymbol{\theta})$. Although $p_1(\boldsymbol{\theta})$ is independent of future states of the sensors, the sensor probability distributions are functions of the future states of the sensors, states controlled by the information theoretic optimization.

III. Methodology

The goal of the search problem is to minimize the uncertainty encompassed in the posterior distribution of the target state, represented here by a particle filter. Regardless of the specific implementation of the particle filter, the method proposed in this work focuses on controlling the vehicles such that they maneuver the sensors to make observations that reduce the uncertainty in the particle set as quickly as possible, distinguishing likely particles from unlikely particles.

This section proceeds by first reviewing particle filters as implemented here. Then a method is developed to compute mutual information directly from the particle filter representation. To improve the efficiency of computing mutual information as the size of the sensor network grows, two decompositions are derived next. These approximations, with analytically quantified error, permit a direct tradeoff between computational complexity and the level of cooperation between vehicles. Finally, the distributed control algorithm applied to these utility functions is presented.

A. Particle Filter

Particle filters are a Monte Carlo method to perform Bayesian estimation. By using this method, it is possible to directly use nonlinear sensor and motion models, non-Gaussian noise models, and non-Gaussian posterior probability distributions. Although particle filters typically incur more computational cost than parametric methods for nonlinear estimation, a well formulated particle filter generally results in a more accurate representation of the solution [14]. The method is presented here for completeness, as an existing technology. Specific algorithms remain an active field of research. For more details, the reader is referred to [14], [27], [30].

Each vehicle approximates $p(\boldsymbol{\theta}_t)$ with an onboard particle filter, incorporating the observations shared by all vehicles, with

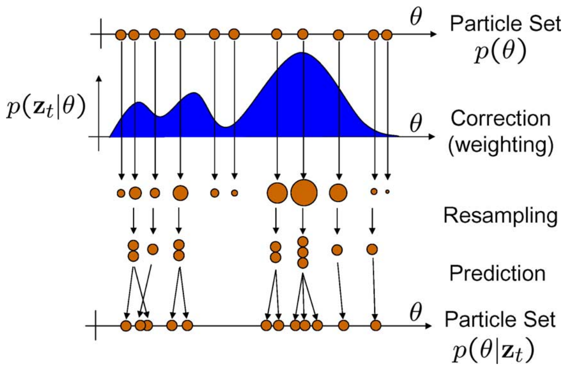

Fig. 3. Graphical depiction of a 1-D particle filter. This non-parametric method approximates Bayes' rule updates, (4). The filter is initialized by drawing *particles* from a prior probability distribution over the state space $p(\boldsymbol{\theta})$. Sensor measurements $\mathbf{z}_t$ and sensor models are used to weight particles according to their likelihood given their states. The particles can then be resampled, according to their weights, to concentrate on regions with high likelihoods. Finally, the particle distribution is predicted for the subsequent time step and future observations are iteratively incorporated [14], [30].

a set of N particles $(\tilde{\boldsymbol{\theta}}^{(i)}_{t,k}, \mathbf{w}^{(i)}_{t,k})$ indexed by k, where $\tilde{\boldsymbol{\theta}}^{(i)}_{t,k} \in \boldsymbol{\Theta}$ is the state of the particle, and $\mathbf{w}^{(i)}_{t,k} \in \mathbb{R}_+$ is the importance weight.[2] The particles represent $p(\boldsymbol{\theta}_t)$ by the probability mass function

$$\hat{p}^{(i)}(\boldsymbol{\theta}_t) = \sum_{k=1}^{N} \mathbf{w}^{(i)}_{t,k} \delta(\boldsymbol{\theta}_t - \tilde{\boldsymbol{\theta}}^{(i)}_{t,k}) \tag{10}$$

where $\delta(\cdot)$ is the Dirac delta function. This approximates $p(\boldsymbol{\theta}_t)$ over intervals in $\boldsymbol{\Theta}$, with convergence results given in [31].

By maintaining a set of particles locally aboard each vehicle, only the observations need to be communicated, as opposed to the values of the entire particle set. The particle filter iteratively incorporates new observations by predicting the state of each particle, updating importance weights with the likelihood of new observations, and then resampling the particles, as depicted in Fig. 3 and described in detail in [27], [30].

This work uses a standard sampling-importance-resampling algorithm [14], [30] with a low variance sampler [14] having time complexity $\mathcal{O}(N)$. Resampling is performed when the effective sample size estimate $N_{eff} = 1/\sum_{k=1}^{N} \left(w^{(i)}_{t,k}\right)^2$ is less than $N/2$[32]. The minimum mean square error (MMSE) estimate is computed using

$$\hat{\boldsymbol{\theta}}^{(i)}_t = \int_{\boldsymbol{\Theta}} \boldsymbol{\theta}_t p(\boldsymbol{\theta}_t) d\boldsymbol{\theta} \approx \sum_{k=1}^{N} \mathbf{w}^{(i)}_{t,k} \tilde{\boldsymbol{\theta}}^{(i)}_{t,k}. \tag{11}$$

B. Determining Mutual Information From Particle Sets

To evaluate the mutual information utility function, (9), it can be expanded as [29]

$$I(\mathbf{z}_t; \boldsymbol{\theta}_t) = H(\mathbf{z}_t) - H(\mathbf{z}_t|\boldsymbol{\theta}_t). \tag{12}$$

[2]The second subscript of any variable denotes the index of the particle to which the variable belongs.

Minimizing the expected posterior uncertainty is equivalent to maximizing the difference between the uncertainty that any particular observation will be made, $H(\mathbf{z}_t)$, and the uncertainty of the measurement model, $H(\mathbf{z}_t|\boldsymbol{\theta}_t)$.

To compute (12) using the particle filter representation, start with the first term,

$$H(\mathbf{z}_t) = -\int_{Z} p(\mathbf{z}_t) \log p(\mathbf{z}_t) d\mathbf{z}. \tag{13}$$

This cannot be directly evaluated because $p(\mathbf{z}_t)$ must be determined from the particle set and sensor model. First, expand the distribution as

$$p(\mathbf{z}_t) = \int_{\boldsymbol{\Theta}} p(\mathbf{z}_t|\boldsymbol{\theta}_t) p(\boldsymbol{\theta}_t) d\boldsymbol{\theta}. \tag{14}$$

Note that when sensor observations are conditionally independent given the target state, a useful decomposition is

$$p(\mathbf{z}_t|\boldsymbol{\theta}_t) = \prod_{j=1}^{n_v} p(\mathbf{z}^{(j)}_t|\boldsymbol{\theta}_t). \tag{15}$$

This is true when sensor noise is uncorrelated and due to local effects at the sensor, as is often the case.

Next, Monte Carlo integration techniques can be used [33]. Substituting (10) into (14) yields the particle filter approximation at the i^{th} vehicle

$$p(\mathbf{z}_t) \approx \sum_{k=1}^{N} \left(\mathbf{w}^{(i)}_{t,k} p(\mathbf{z}_t|\boldsymbol{\theta}_t = \tilde{\boldsymbol{\theta}}^{(\mathrm{i})}_{\mathrm{t,k}}) \right). \tag{16}$$

Remark 1 (Normalizing Weights): The importance weights must be normalized to sum to one prior to Monte Carlo integration. All $w^{(i)}_{t,k}$ must be divided by $\sum_{k=1}^{N} w^{(i)}_{t,k}$.

Substituting (16) into (13) yields the observation entropy of the distribution represented by the particle filter approximation at the i^{th} vehicle

$$\begin{aligned} H(\mathbf{z}_t) \approx -\int_{Z} \Bigg\{ &\left(\sum_{k=1}^{N} \left(\mathbf{w}^{(i)}_{t,k} p(\mathbf{z}_t|\boldsymbol{\theta}_t = \tilde{\boldsymbol{\theta}}^{(\mathrm{i})}_{\mathrm{t,k}}) \right) \right) \\ &\cdot \log \left(\sum_{k=1}^{N} \left(\mathbf{w}^{(i)}_{t,k} p(\mathbf{z}_t|\boldsymbol{\theta}_t = \tilde{\boldsymbol{\theta}}^{(\mathrm{i})}_{\mathrm{t,k}}) \right) \right) \Bigg\} d\mathbf{z}. \end{aligned} \tag{17}$$

This integration can then be performed using an appropriate numerical quadrature technique [34].

Next, similar methods are applied to compute

$$H(\mathbf{z}_t|\boldsymbol{\theta}_t) = -\int_{Z,\boldsymbol{\Theta}} p(\mathbf{z}_t, \boldsymbol{\theta}_t) \log p(\mathbf{z}_t|\boldsymbol{\theta}_t) d\mathbf{z} d\boldsymbol{\theta}. \tag{18}$$

The joint distribution can be expanded using the chain rule

$$p(\mathbf{z}_t, \boldsymbol{\theta}_t) = p(\boldsymbol{\theta}_t) p(\mathbf{z}_t|\boldsymbol{\theta}_t). \tag{19}$$

Substituting (19) into (18) and applying the approximation, (10), yields the conditional observation entropy of the distribution represented by the particle filter at the i^{th} vehicle

$$H(\mathbf{z}_t|\boldsymbol{\theta}_t) \approx -\int_Z \sum_{k=1}^{N} \left\{ \mathbf{w}_{t,k}^{(i)} p(\mathbf{z}_t|\boldsymbol{\theta}_t = \tilde{\boldsymbol{\theta}}_{t,k}^{(i)}) \cdot \log p(\mathbf{z}_t|\boldsymbol{\theta}_t = \tilde{\boldsymbol{\theta}}_{t,k}^{(i)}) \right\} d\mathbf{z}. \quad (20)$$

Thus, the mutual information utility function, (9), can be found by using (17), (20), and (12).

Remark 2 (Independent Distributions): If $p(\mathbf{z}_t)$ and $p(\boldsymbol{\theta}_t)$ are independent distributions, then $I(\mathbf{z}_t;\boldsymbol{\theta}_t) = 0$. To examine (17) and (20) in this limit, consider a sensor with $p(\mathbf{z}_t|\boldsymbol{\theta}_t) = m(\mathbf{z}_t)$, independent of $\boldsymbol{\theta}_t$. Then, (17) approximates $H(\mathbf{z}_t)$ as

$$H(\mathbf{z}_t) \approx -\int_Z m(\mathbf{z}_t) \log(m(\mathbf{z}_t)) d\mathbf{z}. \quad (21)$$

Similarly, $H(\mathbf{z}_t|\boldsymbol{\theta}_t)$ evaluates to the same expression. Therefore, in the limit where $p(\mathbf{z}_t)$ and $p(\boldsymbol{\theta}_t)$ are independent, $I(\mathbf{z}_t;\boldsymbol{\theta}_t)$ given by (12) is zero, the exact value.

Remark 3 (Particle Subsampling): Accuracy and computation time can be traded off by subsampling the particle set to evaluate the objective function (e.g., using low variance resampling). Experimentally, the number of particles required to accurately compute $I(\mathbf{z}_t;\boldsymbol{\theta}_t)$ is typically less than the number required to estimate the posterior distribution.

This optimization remains highly coupled between the n_v vehicles. Next, the degree of cooperation between the vehicles is analyzed to determine a scalable control strategy.

C. Approximately Decoupling Mutual Information

The mutual information between the random variables $\boldsymbol{\theta}_t$ and $\mathbf{z}_t$ quantifies the expected reduction in uncertainty. However, the computational complexity of using a particle set representation to evaluate this quantity grows exponentially with n_z due to integration over each dimension.

We present two approximations to mutual information that allow it to be evaluated in polynomial time with respect to the number of sensors. This makes the network scalable, yet capable of exploiting the descriptiveness of the particle filter. Note that the approximations are general; not specific to particle filters. This section proceeds by first defining the approximations and then quantifying and comparing the errors incurred. First, consider the single-node approximation.

Definition 2 (Single-Node Approximation): This equation approximates the mutual information utility function, (9), for optimization routines onboard the i^{th} vehicle, using

$$V_s^{(i)}(\mathbf{x}_t, \mathbf{u}_t, p(\theta_t)) = I(\mathbf{z}_t^{(i)};\boldsymbol{\theta}_t). \quad (22)$$

This differs from (9) in that only the sensor aboard vehicle i is considered for computing the mutual information.

In this approximation, a sensing node's utility function uses the previous observations of all sensing nodes, but only considers its own future observations. Although the vehicles cooperate through a distributed optimization, their local utility functions do not include the effect of future observations of each other's sensors. This is equivalent to an approximation in the literature that has been applied to linearized, Gaussian estimators (e.g., [9]). The computational complexity of the single-node approximation is constant with respect to n_v.

Second, in a new approximation to improve accuracy, the pairwise interactions of all vehicles are additionally considered. This more accurately captures the effect of group control inputs on mutual information (as will be proven in Theorem 3) with computational complexity linear in n_v. This new technique is the pairwise-node approximation,

Definition 3 (Pairwise-Node Approximation): This equation approximates the mutual information utility function, (9), for optimization routines onboard the i^{th} vehicle using

$$V_p^{(i)}(\mathbf{x}_t, \mathbf{u}_t, p(\theta_t)) = (2 - n_v)\left(I(\mathbf{z}_t^{(i)};\boldsymbol{\theta}_t)\right) + \sum_{\substack{j=1 \\ j\neq i}}^{n_v} \left(I(\mathbf{z}_t^{(i)}, \mathbf{z}_t^{(j)};\boldsymbol{\theta}_t)\right) \quad (23)$$

where $n_v \geq 2$; otherwise (9) is readily used.

Using this approximation, sensing nodes additionally consider the effect of other vehicles' future observations, pairwise, on the utility of their own future observations. Whereas the single-node approximation leads to emergent cooperative behavior from common knowledge of the target state distribution, the pairwise-node approximation makes possible improved cooperation by approximating the effect of future observations of all other sensing nodes on the mutual information.

To quantify the error incurred in these approximations, a preliminary lemma is given for the subsequent theorems.

Lemma 1 (Exchange of Conditioning Variables): The conditioning variables in mutual information can be exchanged, for random variable a, b, and c, using either of

$$I(a;b|c) = I(a;b) - I(a;c) + I(a;c|b), \quad (24)$$
$$I(a;b|c) = I(a;b) - I(b;c) + I(b;c|a). \quad (25)$$

Proof:

$$\begin{aligned} I(a;b) - I(a;b|c) &= H(a) - H(a|b) - H(a|c) + H(a|b,c) \\ &= I(a;c) - I(a;c|b) \end{aligned}$$

proving (24). Equation (25) follows by commuting the order of a and b in $I(a;b)$ and $I(a;b|c)$ above. ■

To quantify the error incurred by the approximations, analytical expressions for the errors are derived and compared. First, consider the single-node approximation.

Theorem 1 (Single-Node Approximation Error): The difference between the single-node approximation for the i^{th} vehicle and the true value of (9) is ϵ_s

$$\epsilon_s^{(i)} = c_s^{(i)} + \sum_{\substack{j=2 \\ j\neq i}}^{n_v} \left(I(\mathbf{z}_t^{(j)};\mathbf{z}_t^{(i)}, \mathbf{z}_t^{(1)}, \ldots, \mathbf{z}_t^{(j-1)})\right) \quad (26)$$

where $c_s^{(i)}$ encompasses the terms that are constant with respect to the i^{th} mobile sensor's control inputs.

Proof: Without loss of generality, consider the case of approximating the mutual information from the perspective of vehicle $i = 1$. The mutual information can be expanded using the chain rule [29], and then rewritten using Lemma 1 to yield

$$I(\boldsymbol{\theta}_t;\mathbf{z}_t) = \sum_{j=1}^{n_v} I(\boldsymbol{\theta}_t;\mathbf{z}_t^{(j)}|\mathbf{z}_t^{(1)},\ldots,\mathbf{z}_t^{(j-1)})$$
$$= \sum_{j=1}^{n_v}(I(\boldsymbol{\theta}_t;\mathbf{z}_t^{(j)}) - I(\boldsymbol{\theta}_t;\mathbf{z}_t^{(1)},\ldots,\mathbf{z}_t^{(j-1)}) + I(\boldsymbol{\theta}_t;\mathbf{z}_t^{(1)},\ldots,\mathbf{z}_t^{(j-1)}|\mathbf{z}_t^{(j)})).$$

Exchanging conditioning variables on the latter two terms using (25)

$$I(\boldsymbol{\theta}_t;\mathbf{z}_t) = V_s^{(1)}(\mathbf{x}_t,\mathbf{u}_t,p(\theta_t)) + c_s^{(1)} + \sum_{j=2}^{n_v}\left(I(\mathbf{z}_t^{(j)};\mathbf{z}_t^{(1)},\ldots,\mathbf{z}_t^{(j-1)}|\boldsymbol{\theta}_t) - I(\mathbf{z}_t^{(j)};\mathbf{z}_t^{(1)},\ldots,\mathbf{z}_t^{(j-1)})\right).$$

with constant $c_s^{(i)} = -\sum_{\substack{j=1\\ j\neq i}}^{n_v} I(\mathbf{z}_t^{(j)};\boldsymbol{\theta}_t)$. Applying the assumption that observations are conditionally independent given the target state, the first term in the summation is zero. This assumption is exact when sensor noise is uncorrelated between vehicles and due to local effects at the sensor. Thus, generalizing to the i^{th} vehicle, the mutual information utility function can be evaluated using (22) with error given by (26). ■

Next, we consider the pairwise-node approximation.

Theorem 2 (Pairwise-Node Approximation Error): The difference between the pairwise-node approximation for the i^{th} vehicle and the true value of (9) is ϵ_p

$$\epsilon_p^{(i)} = \sum_{\substack{j=2\\ j\neq i}}^{n_v}\left(I(\mathbf{z}_t^{(j)};\mathbf{z}_t^{(1)},\ldots,\mathbf{z}_t^{(j-1)}|\mathbf{z}_t^{(i)})\right). \quad (27)$$

Proof: Without loss of generality, consider the case of approximating the mutual information from the perspective of vehicle $i = 1$. The mutual information can be expanded using an application of the chain rule, separating the first term in the summation, and applying the chain rule again

$$I(\boldsymbol{\theta}_t;\mathbf{z}_t) = I(\boldsymbol{\theta}_t;\mathbf{z}_t^{(1)}) + \sum_{j=2}^{n_v}\left(I(\boldsymbol{\theta}_t;\mathbf{z}_t^{(1)},\mathbf{z}_t^{(j)}|\mathbf{z}_t^{(2)},\ldots,\mathbf{z}_t^{(j-1)}) - I(\boldsymbol{\theta}_t;\mathbf{z}_t^{(1)}|\mathbf{z}_t^{(2)},\ldots,\mathbf{z}_t^{(j-1)})\right).$$

Exchanging conditioning variables in the summation using (25), canceling the resulting terms that sum to zero, and splitting the remaining summation yields

$$I(\boldsymbol{\theta}_t;\mathbf{z}_t) = V_p^{(1)}(\mathbf{x}_t,\mathbf{u}_t,p(\theta_t)) + \sum_{j=3}^{n_v}\left(I(\boldsymbol{\theta}_t;\mathbf{z}_t^{(2)},\ldots,\mathbf{z}_t^{(j-1)}|\mathbf{z}_t^{(1)},\mathbf{z}_t^{(j)}) - I(\boldsymbol{\theta}_t;\mathbf{z}_t^{(2)},\ldots,\mathbf{z}_t^{(j-1)}|\mathbf{z}_t^{(1)})\right).$$

Exchanging conditioning variables inside the summation, canceling terms summing to zero, and assuming conditional independence of observations given the target state yields

$$I(\boldsymbol{\theta}_t;\mathbf{z}_t) = V_p^{(1)}(\mathbf{x}_t,\mathbf{u}_t,p(\theta_t)) + \epsilon_p^{(1)}.$$

Thus, the mutual information utility function can be evaluated using (23) with error given by (27). ■

Now consider the effect that this added computational complexity has on the error terms, as a function of the value of the i^{th} vehicle's control inputs.

Theorem 3 (Relative Accuracy of Approximations): The magnitude of the error terms that vary with the i^{th} vehicle's control inputs in the single-node approximation is greater than or equal to the magnitude of the pairwise-node approximation error terms, and equal only when the vehicle's observations are independent of all other vehicles. That is

$$|\epsilon_s^{(i)} - c_s^{(i)}| \geq |\epsilon_p^{(i)}|. \quad (28)$$

Proof: Subtract from the single-node approximation error, (26), the terms that do not vary with the $i^{(th)}$ vehicle's control inputs, $c_s^{(i)}$, and apply the chain rule for mutual information [29]

$$I(\mathbf{z}_t^{(j)};\mathbf{z}_t^{(i)},\mathbf{z}_t^{(1)},\ldots,\mathbf{z}_t^{(j-1)}) = I(\mathbf{z}_t^{(j)};\mathbf{z}_t^{(i)}) + I(\mathbf{z}_t^{(j)};\mathbf{z}_t^{(1)},\ldots,\mathbf{z}_t^{(j-1)}|\mathbf{z}_t^{(i)}). \quad (29)$$

Mutual information is always non-negative, and is zero only if the distributions are independent. So

$$I(\mathbf{z}_t^{(j)};\mathbf{z}_t^{(i)},\mathbf{z}_t^{(1)},\ldots,\mathbf{z}_t^{(j-1)}) \geq I(\mathbf{z}_t^{(j)};\mathbf{z}_t^{(2)},\ldots,\mathbf{z}_t^{(j-1)}|\mathbf{z}_t^{(i)}). \quad (30)$$

The magnitudes of the sums of the left and right sides of this equation, from $j = 1$ to $j = n_v$, are equal to, respectively, the left and right sides of (28). ■

When the sensor measurements are uncorrelated, the single-node approximation yields the same result as the pairwise-node approximation and is computationally faster. However, if the observations are correlated, as is more frequently true, then the pairwise-node approximation yields a closer estimate.

Although the magnitude of the pairwise-node approximation error is less than that of the single-node approximation, it is not possible to guarantee that the optimization is not skewed by some systematic error between the exact solution and the single-node error. However, using the pairwise-node approximation still yields an approximate expected mutual information surpassing what seemed possible using the single-node approximation, and in experiments, the pairwise-node approximation yields better results, as presented in Section IV. In summary, no matter the method used—the exact expression with (12), (17), and (20), the single-node approximation with (22), or the pairwise-node approximation with (23) —the vehicles can evaluate the mutual information utility function, in a decentralized manner, to enable them to cooperatively seek the target. By optimizing this objective function, they actively aim to reduce the uncertainty in their particle filters. By using the single-node approximation, the vehicles can run the local optimization problem faster, and cooperate by trying to reduce the uncertainty of the same posterior distribution. By using the pairwise-node approximation, the computational expense of the objective function is reduced from the full problem, yet the vehicles consider the future observations that can be made collectively—their objective functions reward them such that their combined future observations reduce the uncertainty of the target state as fast or faster than the single-node approximation. Next, we consider how these objective functions are optimized in a distributed manner.

D. Mobile Sensor Network Control

The mobile sensor network control problem is structured as a set of local optimal control problems for each sensing node, coupled through interconnecting constraints. The local optimization problem is formed holding the actions of the other vehicles fixed, using an iterative algorithm based on [35], ensuring convergence to ϵ-feasible solutions that satisfy the necessary conditions for Pareto optimality. The distributed algorithm iterates by communicating interim solutions of control inputs amongst vehicles between local optimizations in a hierarchical, synchronous, or asynchronous manner. To satisfy the interconnecting constraints, a penalty function [36] is defined for each vehicle as

$$P(\mathbf{x}_t, \mathbf{u}_t) = \sum_{m=1}^{n_c^{(i)}} \max(0, g^{(i,m)}(\mathbf{x}_t, \mathbf{u}_t))^{\gamma} \tag{31}$$

where m indexes a set of $n_c^{(i)}$ interconnecting inequality constraints, $g^{(i,m)}$, that affect vehicle i. The penalty function must be zero wherever the constraints are satisfied and must be differentiable. The $n_v - 1$ collision avoidance constraints from (2) are written as

$$\begin{aligned} g^{(i,m)} &= d_{\min} - \|x_{t+1}^{(i)} - x_{t+1}^{(m)}\| \leq 0 \\ &\forall m \in \{1, \ldots, n_v : m \neq i\}. \end{aligned} \tag{32}$$

The penalty function is subtracted from the individual vehicle cost scaled by penalty parameter β, varying the tradeoff between constraint violation and the information theoretic cost, with an update $\beta := \alpha\beta$ at each iteration, where $\alpha \in (0,1)$ is a design parameter. The local optimization problem based on the single-node approximation, (22), is

$$\boxed{\begin{aligned} &\textit{Single-Node Local Optimization Program:} \\ &\underset{\mathbf{u}_t^{(i)} \in U}{\text{maximize}} \quad V_s^{(i)}(\mathbf{u}_t, \mathbf{x}_t, p(\boldsymbol{\theta}_t)) - \tfrac{1}{\beta} P(\mathbf{x}_t, \mathbf{u}_t) \\ &\text{subject to} \quad \mathbf{x}_{t+1} = f_t(\mathbf{x}_t, \mathbf{u}_t) \\ &\qquad\qquad\quad \mathbf{z}_t = h(\mathbf{x}_{t+1}, \boldsymbol{\theta}_t, \boldsymbol{\eta}_t). \end{aligned}} \tag{33}$$

The argument for this optimization program is the local control input. Other control inputs in the penalty function arguments are the current desired values communicated by other vehicles.

The single-node approximation will not vary with the control inputs of other vehicles, hence agreement between vehicles on the correct control actions for the group is not required. Only the collision avoidance constraint must be satisfied. For the pairwise-node approximation, (23), the control inputs of all vehicles affect the objective function, $V_p^{(i)}$, hence slack variables must be added to decouple the local sensor costs, resulting in additional interconnecting constraints to include in the penalty function. Define the slack variable $\tilde{\mathbf{u}}_t^{(i)}$ as the vector of all sensors' control inputs computed by the i^{th} sensor. Agreement among mobile sensing nodes on $\tilde{\mathbf{u}}_t^{(i)}$ is realized through the penalty function enforced constraint

$$\tilde{\mathbf{u}}_t^{(i)} = \tilde{\mathbf{u}}_t^{(j)} \quad \forall i, j \in \{1, \ldots, n_v : j \neq i\}. \tag{34}$$

The pairwise-node local optimization program is defined analogously to the single-node local optimization program, with optimization instead over the entire control vector $\tilde{\mathbf{u}}_t^{(i)} \in U$.

Potential extensions include consideration of inter-agent coupling [37]. It is also interesting to consider cases where there is not global connectivity, communication is intermittent, or bandwidth is limited. These are topics of current research.

As described in Algorithm 1, for a hierarchical implementation the vehicles are ordered in a fixed manner. Initial solutions are determined locally ignoring interconnected constraints. Then, prior to local optimization, the relative weight of the penalty function with respect to the local cost is increased by a factor $\alpha \in (0,1)$ and $\beta := \alpha\beta$, increasing the penalty of violating the interconnecting constraints gradually as the vehicles iterate. Each vehicle, starting with 1, solves the local information-seeking optimization problem with the current preferred solution and penalty parameter, and subsequently passes that solution and parameter on to the next vehicle. The optimization concludes when the solution agreed to is within $\epsilon > 0$ of feasible and the local cost functions satisfy an appropriate convergence criteria.

Algorithm 1 Single Time Step Distributed Optimization

1: Define $\mathbf{x}_t$

2: Initialize $\mathbf{u}_t$ or $\tilde{\mathbf{u}}_t$

3: **repeat**

4: $\beta \leftarrow \alpha\beta$

5: **for** $i = 1$ to n_v **do**

6: Transmit $\mathbf{u}_t$ or $\tilde{\mathbf{u}}_t$ to vehicle i

7: Perform local optimization at vehicle i

8: Update $\mathbf{u}_t^{(i)}$ or $\tilde{\mathbf{u}}_t^{(i)}$ for vehicle i

9: **end for**

10: **until** Convergence criteria satisfied

This algorithm ensures that all vehicles, with control constraints, maintain collision-free operation while maximizing the information gain at each time step. Through the single-node and pairwise-node approximations, the algorithm can be computed in real-time and implemented for many actual scenarios (e.g., convergence of each iteration in the examples of Section IV took fractions of seconds). Real-time performance is indeed a relative concept, depending on problem complexity, computation power, network size, communication capabilities, and measurement rate. However, the approximations presented provide objective functions that have polynomial computational complexity with respect to the number of vehicles.

(a)

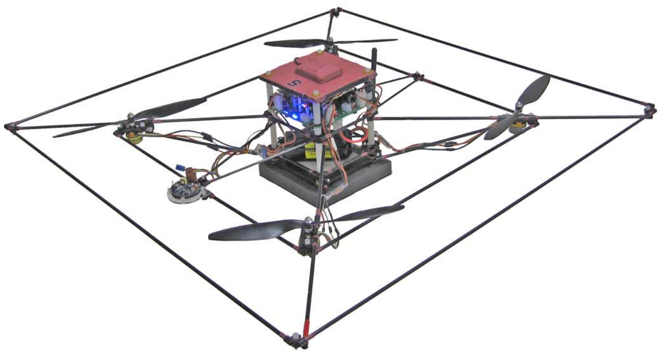

(b)

Fig. 4. (a) Two quadrotor helicopters from the Stanford Testbed of Autonomous Rotorcraft for Multi-Agent Control (STARMAC), hovering at GPS waypoints. The simulations use dynamic models of these (b) vehicles.

IV. Information-Seeking Examples

The proposed techniques are explored for three sensing modalities. The first modality, bearings-only sensing, allows comparison to previous work. Advantages are seen in using a particle filter over a linearized filter when there is large initial uncertainty. The second modality, range-only sensing, is prone to bias and divergence when using standard linearized methods, but demonstrates intuitive results when using particle filter methods. The final modality, sensing the magnetic field of a rescue beacon, demonstrates a problem that cannot be solved by linearized methods because the beacon orientation, a random variable on a periodic domain, has large uncertainty during most of the search. In order to capture the effects of future observations, it is necessary to plan using mutual information methods with particle filters.

The vehicle model for these examples is based on the STARMAC quadrotor helicopters, shown in Fig. 4 and detailed in [6]. Note that any choice of vehicle or portable device could be used for the algorithms developed. The dynamics of a quadrotor helicopter can be approximated as those of a point mass capable of accelerating in any direction, subject to constraints. For safety, a velocity constraint is also imposed. Further, they must maintain separation. Parameters for the simulations are given in Table I.

TABLE I
Simulation Parameters and Legend

Category	Parameter	Value
Vehicle	Type	Quadrotor
	Speed limit	2 $\mathrm{m/s}$
	Acceleration limit	0.2 $\mathrm{m/s^2}$
	Minimum separation, $\bar{d}$	3 m
Particle Filter	Search area	40×40 m square
	Prior, $p(\theta_0)$	Uniform over $\boldsymbol{\Theta}$
	Number of particles, N	2000
Plot	Particle darkness	$\propto w_{t,k}^{(1)}$
	True target location	Square icon
	MMSE estimate	X icon
	Curve trailing vehicles	History of trajectory

In the each of the following three examples, the measurement model is first presented. Then, the expected behavior of the information seeking sensor network is determined for comparison for an accurately known target location using a linearized measurement model. This predicted behavior can differ from the simulated system, as the linearization used for analysis simplifies effects that are fully captured by particle filter mutual information methods. However, it validates the particle filter methods when the approximation is reasonable, and otherwise permits the particle filter methods to be compared and contrasted to linearized, Gaussian methods. Finally, simulation results using particle filter mutual information methods are presented.

A. Bearings-Only Sensing

For this example, consider sensors that measure the direction to the target, such as cameras [11] or directional antennae [3]. We will demonstrate that the non-Gaussian posterior probability distribution can be captured using the particle filter representation and directly used by the mutual information utility function. Results using the single-node approximation show that emergent behavior due to prior information can be sometimes beneficial, but sometimes counterproductive. The pairwise-node approximation yields more consistent behavior resulting in better performance, on average. By using particle filter methods, the bias, underestimated covariance, and divergence associated with EKFs [15], [16], [38], can be avoided. No divergence was encountered in simulations of the methods, and the mutual information optimization successfully maneuvers the vehicle to extract information about the probability distribution represented by the particle set.

1) Measurement Model: Consider searching for a target in the xy-plane. The location of the i^{th} search vehicle at time t is $(x_t^{(i)},\ y_t^{(i)})^T$, components of $\mathbf{x}_t^{(i)}$. The state of the target is its location $\boldsymbol{\theta} = (x_m,\ y_m)^T$. The bearing measurement model is

$$h_b^{(i)}(\mathbf{x}_t^{(i)}, \boldsymbol{\theta}, \boldsymbol{\eta}_t^{(i)}) = \arctan\left(\frac{y_m - y_t^{(i)}}{x_m - x_t^{(i)}}\right) - \psi_t^{(i)} + \boldsymbol{\eta}_t^{(i)} \quad (35)$$

where h_b is the model of the bearing measurement with noise, as shown in Fig. 5, $\psi_t^{(i)}$ is the i^{th} vehicle's heading and $\boldsymbol{\eta}_t^{(i)} \sim \mathcal{N}(0, \sigma_b^2)$ is the measurement noise. Although any measurement model could be used for this particle filter implementation, such as one including pixel noise in a camera, or one including signal attenuation with range for a directional antenna, the additive noise model allows comparison to previous work (e.g., [9], [11],

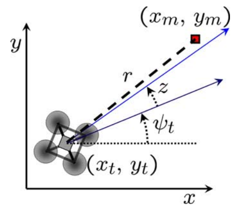

Fig. 5. Bearings-only measurement model, where z is a measurement of the direction from the position of the sensor $(x_t^{(i)},\ y_t^{(i)})^T$ to the position of the target $(x_m^{(i)},\ y_m^{(i)})^T$. It differs from the true direction due to additive noise, given by (35). Examples sensors include cameras and directional antennae.

[12]). The variance is σ_b^2, which for simplicity is chosen to be the same for all sensors.

2) Predicted Behavior: For bearings-only sensors the optimal control actions for a linearized, Gaussian approximation of the system provide a reasonable prediction of the behavior of the optimal system, with some exceptions. With this approximation, trends in optimal sensor placement and the effect of increasing n_v can be derived. Let $p(\boldsymbol{\theta}_t)$ be approximated as Gaussian with mean $(\hat{x}_m,\ \hat{y}_m)^T$ and covariance Σ. The Jacobian of (35) is

$$J_b^{(i)} = \frac{1}{r^{(i)}}\left[\sin\xi^{(i)} \quad -\cos\xi^{(i)}\right] \tag{36}$$

where $\xi^{(i)} = \arctan 2\left(\hat{y}_m - y_t^{(i)},\ \hat{x}_m - x_t^{(i)}\right)$ and $r^{(i)} = \sqrt{\left(\hat{x}_m - x_t^{(i)}\right)^2 + \left(\hat{y}_m - y_t^{(i)}\right)^2}$. The goal is to minimize the conditional entropy, as in (5). Using the entropy formula for Gaussians [29], and the covariance update for an EKF [14], the conditional entropy for the linearized problem is

$$\begin{aligned} &H(\boldsymbol{\theta}_t|\mathbf{z}_t) \\ &= \frac{1}{2}\log\left((2\pi e)^2\left|\left(\Sigma^{-1} + \sum_{i=1}^{n_v} J_b^{(i)T}\left(\sigma_b^2\right)^{-1} J_b^{(i)}\right)^{-1}\right|\right) \end{aligned} \tag{37}$$

where

$$J_b^{(i)T}\left(\sigma_b^2\right)^{-1} J_b^{(i)} = \frac{1}{\sigma_b^2\left(r^{(i)}\right)^2}\begin{bmatrix}\sin^2\xi^{(i)} & -\frac{\sin 2\xi^{(i)}}{2} \\ -\frac{\sin 2\xi^{(i)}}{2} & \cos^2\xi^{(i)}\end{bmatrix}. \tag{38}$$

To minimize the uncertainty, (37), it is equivalent to maximize

$$U_b^{(i)}(\boldsymbol{\xi}, \mathbf{r}) = \left|\Sigma^{-1} + \sum_{i=1}^{n_v} J_b^{(i)T}\left(\sigma_b^2\right)^{-1} J_b^{(i)}\right|. \tag{39}$$

This provides two insights into the behavior of information seeking bearings-only sensors. First, as $r^{(i)}$ decreases, $U_b^{(i)}(\boldsymbol{\xi}, \mathbf{r})$ increases—it is beneficial to be close to the target. This is due to the decreased effect of additive direction noise at close range—an effect noticeable in our own vision. Note that as $r^{(i)} \to 0$, the true Bayesian posterior probability distribution has nonzero uncertainty, whereas linearization error in the EKF causes $U_b^{(i)}(\boldsymbol{\xi}, \mathbf{r}) \to \infty$. If a linear estimator incorporates a measurement made at the mean, the most informative location, the covariance of the estimate becomes singular. To observe a second insight, consider the case in which values of $r^{(i)}$ are equal and nonzero for all i. An analytical solution for optimal values for $\xi^{(i)}$ can be found when $\Sigma = \sigma^2 I$, where σ is the standard deviation in the target state estimate in both axes and I is a 2×2 identity matrix. By taking the gradient of (39), the optimal values of $\xi^{(i)}$ can be shown to be those that satisfy

$$\sum_{i=1}^{n_v}\cos 2\xi^{(i)} = 0 \quad \text{and} \quad \sum_{i=1}^{n_v}\sin 2\xi^{(i)} = 0. \tag{40}$$

Thus, two solutions always satisfy (40), 1) spacing the vehicles with equal angles of π/n_v, and 2) grouping all vehicles into pairs or triplets that are at 90° or 60°, respectively. For $n_v > 4$, a continuum of other solutions exist that achieve minimum conditional entropy. Note that $\cos 2\xi^{(i)} = \cos(2\xi^{(i)} + n\pi)\forall n \in \mathbb{Z}$, so optimally configured vehicles may be on either side of the target with the same benefit—a consequence of the linearization. The complete optimal solution, then, causes the vehicles to fan out to satisfy the optimal direction criteria, and approach the origin, due to the $1/r^{(i)}$ perspective effect.

To determine the benefit of increasing n_v for optimally spaced vehicles, (37) can be simplified using (40), with all vehicles at the same range, $r^{(i)} = r$. Then

$$H(\boldsymbol{\theta}_t|\mathbf{z}_t) = \frac{1}{2}\log\left((2\pi e)^2\left(\frac{1}{\sigma^2} + \frac{n_v}{2\sigma_b^2 r^2}\right)^2\right). \tag{41}$$

As more sensors are added to the network, they increase performance logarithmically. Increasing n_v is equivalent to proportionally decreasing the σ_b^2. The worst case can similarly be computed, for the configuration in which all vehicles are at the same angle with respect to the target

$$H(\boldsymbol{\theta}_t|\mathbf{z}_t) = \frac{1}{2}\log\left((2\pi e)^2\frac{1}{\sigma^2}\left(\frac{1}{\sigma^2} + \frac{n_v}{\sigma_b^2 r^2}\right)\right). \tag{42}$$

Consider the ratio of arguments in the log expressions in (41) and (42). The ratio of the best configuration to worst is

$$\kappa = 1 + \frac{n_v^2}{4\sigma_b^4 r^4 p^{-1}\left(\frac{1}{\sigma^2} + \frac{n_v}{\sigma_b^2 r^2}\right)}. \tag{43}$$

As n_v increases, κ increases—cooperation has more benefit. As the prior uncertainty σ decreases, so does κ, decreasing the benefit of cooperation as the target is better localized.

The patterns of cooperation given by (40) will be apparent in the results using particle filters, as will the benefits of approaching the expected target location. However, the particle filter will be shown to handle nonlinear effects for measurements near the target, rather than risking divergence due to linearization error. The logarithmic benefit of increasing n_v is apparent in the Monte Carlo results.

3) Particle Filter Results: Bearings-only simulations were run with the particle filter mutual information utility functions to determine the empirical behavior of the algorithms, as shown in Fig. 6, and to obtain Monte Carlo results. The uniform prior probability distribution over the search region represents the prior knowledge that the target is contained in the region, with complete uncertainty of its location within.

Simulated sensor noise was $\sigma_b = 0.3$ radians, as might be found in a directional antenna. This large noise exacerbates the effect of large uncertainty, nonlinearities, and non-Gaussian

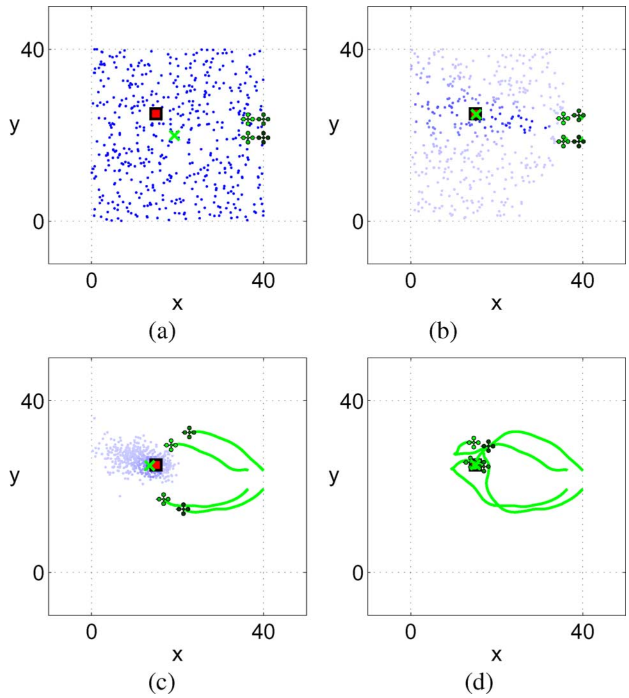

Fig. 6. Simulation of bearings-only target search with four mobile sensors using the particle filter distribution to compute mutual information, and the pairwise-node approximation for distributed control. By directly using the particle filter distribution, there is no bias from linearization, as there is in an EKF. The vehicles spread out around the particle distribution, due to the mutual information utility function, with two pairs spaced apart with respect to the mean as predicted in (40). They approach the expected target location, *only* to gain the maximum information possible. See Table I for simulation parameters and the legend. (a) $t = 0$ s. (b) $t = 3$ s. (c) $t = 22$ s. (d) $t = 50$ s.

posterior distributions to demonstrate the capabilities of the proposed methods. The methods performed equally well with $\sigma_b = 0.01$ radians. Particle deprivation due to low noise was not encountered, though for sufficiently low noise this must be considered [14].

Empirically, it was observed that the particle filter based algorithms result in the rapid localization of the target. These results were consistent for a large number of trial runs, as demonstrated by Monte Carlo results. Sets of 1000 trials were performed for several sizes of networks, with both the single-node and pairwise-node approximations. As shown in Fig. 7(a), the use of the pairwise-node approximation resulted in a reduced time-to-convergence compared to the single-node approximation, on average. The pairwise-node approximation also yielded more consistent performance than the single-node approximation, shown by narrower error bands. This demonstrates the benefit of considering the effects vehicles have on one another while performing the optimization, rather than relying on emergent behavior for vehicle cooperation.

The result of using the pairwise-node approximation for an increasing number of vehicles is shown in Fig. 7(b). The particle filter based information seeking algorithm successfully exploits the additional availability of sensors. The time-to-convergence is reduced, on average, as vehicles are added to the fleet. Next, the use of range-only sensors is analyzed.

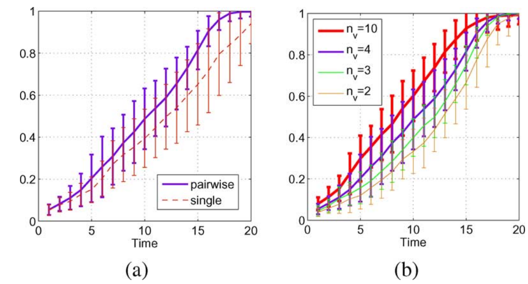

Fig. 7. Mean and quartile bars of the probability that the true target state is within 1 m of the MMSE estimate, for sets of 1000 trials of bearings-only target localization. The difference between the single-node and pairwise-node approximations are shown in (a), with $n_v = 4$. The pairwise-node results are more predictable and result in better expected performance. The effect of utilizing more sensors is shown in (b), comparing the effect of using the pairwise-node approximation for varying number of search vehicles.

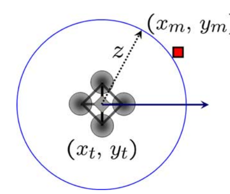

Fig. 8. Range-only measurement model where z is a measurement of the distance from the position of the sensor $(x_t^{(i)}, y_t^{(i)})^T$ to the position of the target $(x_m^{(i)}, y_m^{(i)})^T$. It differs from the true range due to additive noise, given in (44). An example of such a measurement is the time of flight of wireless communication signals.

B. Range-Only Sensing

For this example, we consider sensors that measure the distance to the target, using sensors such as wireless communication devices [4]. In addition to avoiding the problems associated with EKFs described previously, the use of particle filters makes it possible to quantify effects on information gain not possible with a linearized method. Although in the linearized model the optimal range to the target will be shown to be inconsequential for the selected model, the particle filter information formulation finds an optimal range, due to minimum and maximum ranges for the sensor, an effect that cannot be captured by the linearized model.

1) Measurement Model: Again, consider searching for a target in the xy-plane, with the same states as the previous, bearings-only, example. The range measurement model is

$$h_r^{(i)}(\mathbf{x}_t^{(i)}, \boldsymbol{\theta}, \boldsymbol{\eta}_t^{(i)}) = \sqrt{\left(x_m - x_t^{(i)}\right)^2 + \left(y_m - y_t^{(i)}\right)^2} + \boldsymbol{\eta}_t^{(i)} \tag{44}$$

where h_r is the model of the range measurement with noise, as shown in Fig. 8, $\boldsymbol{\eta}_t^{(i)} \sim \mathcal{N}(0, \sigma_r^2)$ is the measurement noise. Although any measurement model could be used, such as noise proportional to range, due to clock drift, the additive noise model is chosen to permit comparison with other work (e.g., [10]). This sensor lacks directional information, hence a single measurement provides an axisymmetric probability distribution of potential target locations.

2) Predicted Behavior: To gain insight into the behavior of the optimally controlled system, again consider the case of an accurately localized target, with a probability distribution well approximated as Gaussian having a covariance matrix equal to a scaled identity matrix. In this condition, the optimal placement of sensors can be solved for, as was done for the bearings-only sensor in Section IV-A. The Jacobian of the sensor model is

$$J_r^{(i)} = [\cos\xi^{(i)} \quad \sin\xi^{(i)}] \tag{45}$$

where ξ is the angle from the i^{th} vehicle to the mean of the target estimate, as in Section IV-A. The uncertainty following a sensing action is

$$H(\boldsymbol{\theta}_t|\mathbf{z}_t) = \frac{1}{2}\log\left((2\pi e)^2 \left|\left(\Sigma^{-1} + \sum J_r^{(i)T}\left(\sigma_r^2\right)^{-1} J_r^{(i)}\right)^{-1}\right|\right) \tag{46}$$

where Σ is the covariance of the target state distribution. Unlike the bearings-only sensor, the posterior uncertainty is not a function of range, in this linearized case. Therefore, only the direction from the target to the vehicles need be optimized. Numerical solutions show an expected behavior—optimal solutions tend to cluster near the elongated axis of the confidence ellipse corresponding to any posterior distribution. If the posterior distribution has equal uncertainty in the x and y directions, then the optimal angles for the bearings-only sensors, given by the conditions of (40), are also the optimal angles for range-only sensors. Either sensor type provides measurements that can be used to "triangulate" a measurement—they are simply providing measurements rotated by 90° from each other—though there is no scaling due to perspective for a range-only sensor. However, particle filters capture the effect of saturation of the sensor and the curvature of the range measurements. The actual range of the range-only sensors is, in fact, important.

3) Particle Filter Results: Range-only simulations were run with the particle filter mutual information utility function and pairwise-node approximation to determine the empirical behavior of the algorithms, and evaluate how the mutual information utility of measurements vary with sensing locations. The sensor has additive noise of $\sigma = 5$ m, a relatively large value for the scale of the search space. This demonstrates the ability of the algorithm to model and react to large uncertainty and non-Gaussian posterior distributions. The maximum range for results presented here is 56 m, enabling comparison with previous work by ensuring that maximum range measurements are unlikely, although the sensor model does consider the effect when it occurs, and has been demonstrated to perform well in similar simulations with maximum ranges of 5 m, 10 m, and 20 m.

The particle filter based algorithms again result in rapid localization of the target, despite complete prior uncertainty over the search region, as shown in a typical result in Fig. 9, using four vehicles with the pairwise-node approximation. Again, the consistent ability of the mobile sensor network to localize the target demonstrates the capabilities of the proposed methods. As expected from the predictions above, the vehicles fan out. The mutual information objective function indicates they will gain the most information in this manner.

The linearized approximation predicts that distance between the sensors and the target is unimportant for this sensor, unlike the bearings-only scenario. However, the vehicles converge to a standoff distance. Differences between the prediction using the linearized approximation and the more accurate particle filter method are highlighted by the comparing available mutual information in Fig. 10, where contours of the mutual information objective function are plotted for an observation from any point. These differences arise from effects that are eliminated by linearization and Gaussian estimation. For instance, there are important nonlinearities. The range-only sensor saturates; a range less than zero would be non-physical, and the maximum is finite. In the example shown in Fig. 10, the sensor limits are 0 to 56 m. Also, effects of the structure of the distribution are captured. It may be ring-like or multimodal. This is not captured by the linearized method. Finally, there is the effect of curvature when interpreting range measurements. This cannot be captured using a linearized method, but is inherently part of the particle filter method. Now, consider a third and final sensor, rescue beacons.

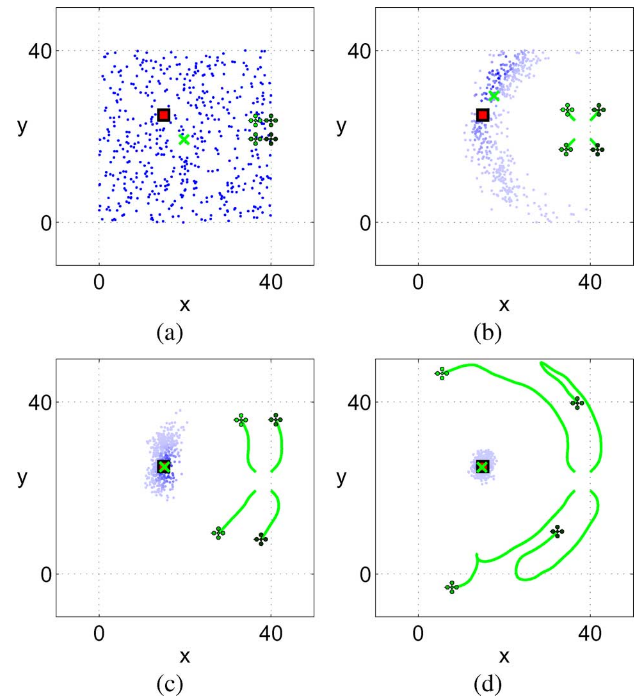

Fig. 9. Range-only target localization with 4 mobile sensors (quadrotor helicopters) using the particle filter distribution to compute mutual information and the pairwise-node approximation for distributed control. The vehicles spread out along the ring of particles, and then fan out at optimal distances to the target, according to the minimum and maximum range of their sensors. Approaching the target would be a sub-optimal solution for these sensors. See Table I for simulation parameters and the legend. (a) $t = 0$ s. (b) $t = 5$ s. (c) $t = 15$ s. (d) $t = 50$ s.

C. Rescue Beacon Sensing

For this example, we consider a sensing modality for which EKFs are prone to failure—sensing the avalanche rescue beacon of a victim buried in snow due to an avalanche. The beacon uses a modulated magnetic dipole with a field that can be measured by beacon receivers. Both the position and orientation of the beacon are unknown, adding complexity beyond the sensors of the previous sections. The search is currently performed by individual rescuers using a rehearsed search pattern—a complex activity requiring professional training to be effective [39]. Rapid

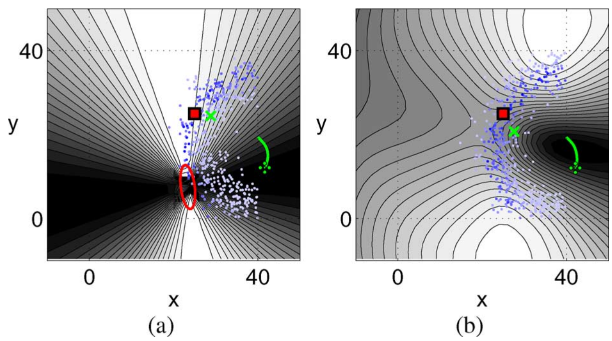

Fig. 10. Using the particle filter to directly compute available mutual information captures effects not possible with a linear Gaussian approximation, such as the saturation of measurements at the near and far limits of the sensor's range. The mutual information contours, for moving to any point at the subsequent time step, are shown (a) using a linear, Gaussian approximation, with an EKF, versus (b) using a particle filter. The brighter the contour, the more information is available. The $1-\sigma$ ellipse of the EKF is shown in (a). In both examples, the vehicle is controlled using the particle filter mutual information, leading to similar trajectories. The plotted particles, etc., are as described in Fig. 6.

localization is essential—in one study, odds of survival were 92% for victims unburied within 15 minutes, but dropped to 30% after 35 min [40]. Particle filters are well suited for this application. Sum-of-Gaussian filter have also been used, with initialization using the first measurement [41]. An approach using a Rao-Blackwellized particle filter performed poorly in simulations [41].

We demonstrate the use of particle filter techniques to estimate the posterior probability distribution and control the vehicles using the particle filter distribution, such that they maximize the rate at which they acquire information about the victim's location. We derive the expected behavior in limited situations by linearizing the measurement model. Due to the periodic domain, the information in the linearized model is only accurate when the target is well localized. This enables validation of the particle filter implementation under that circumstance, toward the conclusion of the search. The particle filter methods handle the automatic acquisition of information during all stages of the search.

1) Measurement Model: The rescue beacon system uses measurements of the magnetic dipole emitted by a loop antenna modulated at 457 kHz, a frequency that penetrates snow and water, and is not reflected by rock [42]. The magnetic field of a modulated electromagnetic source $B:\mathbb{R}^3\rightarrow\mathbb{R}^3$ is derived in [43], and shown in Fig. 11. Given the modulation frequency and range of rescue beacons, the near-field formula for the magnetic field is appropriate [42], [43]. Measurements are made of the toroidal near-field at spherical coordinates $(r^{(i)},\phi^{(i)},\alpha^{(i)})$ with respect to the antenna, where $r^{(i)}$ is the range, $\phi^{(i)}$ is the rotation angle about the axis of the antenna, and $\alpha^{(i)}$ is the elevation angle from the plane of the antenna loop, in the right-hand sense, as shown in a two dimensional cross-section in Fig. 12. The magnetic field is [43]

$$\mathbf{B}=\frac{m}{2\pi\left(r^{(i)}\right)^3}\left((2\sin\alpha^{(i)})\mathbf{e}_r-(\cos\alpha^{(i)})\mathbf{e}_\alpha\right) \quad (47)$$

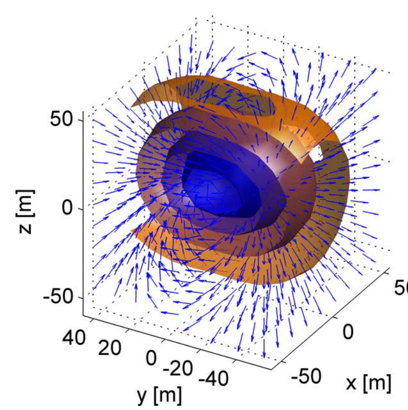

Fig. 11. Rescue beacon magnetic field, as given in (47). Cross section of isosurfaces of field strength is shown, with arrows depicting local magnetic field orientation. The transmitter antenna is at the origin, with its antenna parallel to the y-axis.

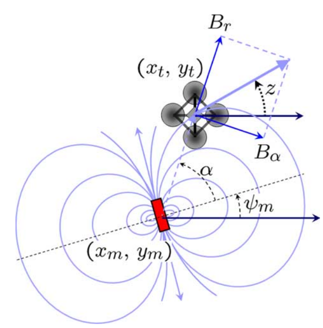

Fig. 12. Rescue beacon measurement model, in two dimensions, with the transmitter antenna axis lying along the xy-plane at (x_m, y_m) with orientation ψ_m. The measurement z is the local orientation of the magnetic field vector in the plane of the receiver, with additive noise, given by (48). The field has components B_r and B_α from (47). The mobile sensor, at time t, is at position (x_t, y_t).

where the magnitude of the dipole moment is $m=I_0\pi r_a^2 n_w$, I_0 is the amplitude of the antenna loop current, r_a is the radius of the antenna loops, n_w is the number of windings, and $\mathbf{e}_r$ and $\mathbf{e}_\alpha$ are unit vectors of the spherical coordinate frame in the positive r and negative α directions, respectively. The sensor measures the orientation of the magnetic field line projected onto the plane in the receiver containing two orthogonal receiver antennae. The angle is computed using the $\arctan$ of the ratio of the measurements on each axis.

For purposes of this simulation, consider a search for a rescue beacon in two dimensions, with its axis known to lie in the horizontal plane, with unknown heading angle ψ_m. The state of the target is $\theta=(x_m,\, y_m,\, \psi_m)^T$, a three dimensional state. Note that it is simple to include the target's altitude and pitch to solve the true problem using the particle filter framework, but the three degree of freedom model used in this paper provides more easily visualized results. The measurement equations can then be written in terms of the magnetic field direction at a receiver

$$h_a^{(i)}\left(\mathbf{x}_t^{(i)},\boldsymbol{\theta},\eta_t^{(i)}\right)=\xi^{(i)}-\arctan\left(2\cot(\alpha^{(i)})\right)+\eta_t^{(i)} \quad (48)$$

where h_a is the modeled value of the noisy magnetic field orientation measurement z as shown in Fig. 12, $\alpha^{(i)} = \xi^{(i)} - \psi_t$, and $\eta_t^{(i)} \sim \mathcal{N}(0, \sigma_a^2)$ is the measurement noise.

2) Predicted Behavior: To gain insight into the behavior of the optimally controlled system, again consider the case of an accurately localized target, with a probability distribution that can be approximated as Gaussian, with a covariance matrix equal to a scaled identity matrix. In this condition, we can analytically solve for the optimal placement of the sensors, as done for sensors in previous sections. The Jacobian of $h_a^{(i)}$ is

$$J_a^{(i)} = \frac{1}{3\left(\lambda^{(i)}\right)^2 + \left(r^{(i)}\right)^2} \begin{bmatrix} \frac{\sin(\xi^{(i)})}{r^{(i)}} \left(\left(r^{(i)}\right)^2 - 3\left(\lambda^{(i)}\right)^2\right) \\ \frac{\cos(\xi^{(i)})}{r^{(i)}} \left(3\left(\lambda^{(i)}\right)^2 - \left(r^{(i)}\right)^2\right) \\ 2\left(r^{(i)}\right)^2 \end{bmatrix}^T \tag{49}$$

where $\lambda^{(i)}$, the lateral distance between the mean of the estimated antenna axis and the measurement point, is

$$\lambda^{(i)} = r^{(i)} \cos \alpha^{(i)}. \tag{50}$$

The optimal sensing utility function can be found using (39) by replacing $J_b^{(i)}$ with $J_a^{(i)}$. High prior uncertainty in orientation yields a utility function similar to a range-only sensor, with the optimal relative angle being along the axis of the sensor. Low prior uncertainty in orientation yields a utility function similar to a bearings-only sensor. Unlike the bearings-only or range-only sensors, few additional generalizations can be drawn from the linearized model, due to its complexity. The mutual information contours for the linearized results were compared to those for the particle filter methods. Although the results match for low uncertainty, unimodal posterior probability distributions, they were found to vary substantially for more typical particle distributions encountered during simulated searches, with multiple modes, and high uncertainty.

3) Particle Filter Results: Rescue beacon simulations were run with the particle filter mutual information utility function and the pairwise-node approximation to show the empirical behavior of the algorithms, and evaluate how the mutual information utility function evolves as the problem converges. In addition estimating the search target's position, the orientation must be estimated. To simplify presentation, the simulated searches were performed using three degrees of freedom as in (48). The sensors measure the local magnetic field line orientation with an additive noise of $\sigma_a = 0.7$ radians. The prior distribution of orientations was uniform over $[0, 2\pi)$. Other simulation parameters are in Table I.

As shown in Fig. 13, the proposed method quickly localizes the target. At first, the vehicles fan out. They proceed to move to locations that reinforce one another's measurements. The behavior is substantially more complicated than that required for range or bearing sensors. The posterior distribution, visualized by the particles, demonstrates the ability of this method to handle complicated posterior beliefs. It successfully exploits the structure of the probability distribution to reduce uncertainty. The four vehicles cooperate in a distributed, computationally efficient manner.

To visualize the optimization being performed aboard the vehicles, Fig. 14 shows the mutual information available for an observation from any point, for one vehicle with $\sigma_a = 0.3$ radians. The vehicle initially is driven away from where the initial measurements were made, as to not make redundant measurements. The low region for mutual information, in the simulated scenario, follows the direction of the field line that was already measured—maximum information can be gained by initially moving orthogonally to the measured field line. Note that this differs from a common method of trained rescuers, who follow the field line direction to compensate for a lack of georeferenced measurements. As the search progresses, and the particle set gains more structure, sometimes multimodal, the contours evolve guiding the vehicle to the best available measurements.

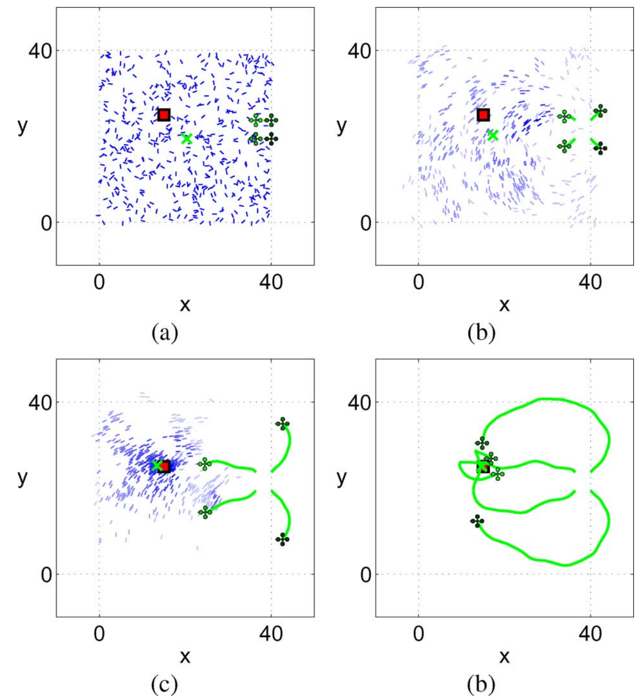

Fig. 13. Rescue beacon localization with 4 sensors using the particle filter distribution to compute mutual information and the pairwise-node approximation for distributed control, simulating the search for a victim buried in an avalanche. The target's orientation is $\psi_m = \pi/4\,\mathrm{radians}$. The orientation of each particle indicates the orientation of its estimate. The vehicles fan out with respect to the particle distribution, as it evolves, and then approach the expected target location, *only* to gain more information about its location. See Table I for simulation parameters and the legend. (a) $t = 0$ s. (b) $t = 5$ s. (c) $t = 15$ s. (b) $t = 50$ s.

The effect of the pairwise-node approximation versus the single-node approximation is visualized in a zoomed in contour plot in Fig. 15. The contours depict the mutual information utility function for placement of a second vehicle, given that a vehicle exists in the location shown. The single-node approximation is not effected by the existing vehicle, whereas the pairwise-node approximation leads to the cooperative behavior of the vehicles fanning out, as appropriate for the depicted rescue beacon search.

V. Conclusion

A set of methods was developed to enable information-theoretic distributed control of a mobile sensor network, based on estimation by particle filters, to search for a target. Although particle filters have higher computational cost than parametric approximation methods, they provide superior descriptiveness of

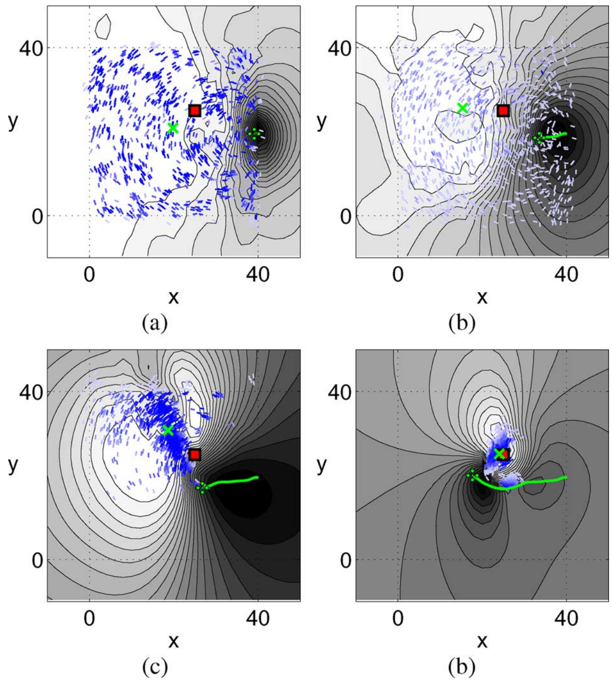

Fig. 14. Using the particle filter to directly compute available mutual information captures effects not possible with a linear Gaussian approximation, such as the spatially varying orientation in the posterior distribution, and multiple modes. The plots show the evolution of the available mutual information, as measurements are collected by a single mobile sensor to localize a rescue beacon, using the exact mutual information utility function. The contours plotted in the background are the available mutual information for measurements from any point. The mobile sensor's control input moves the vehicle to the location with maximal mutual information, subject to constraints. The plotted particles, etc., are as described in Fig. 13. (a) $t = 3$ s. (b) $t = 9$ s. (c) $t = 16$ s. (b) $t = 26$ s.

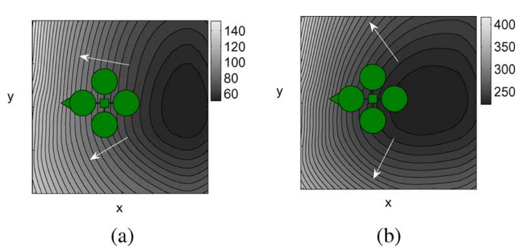

Fig. 15. Comparison of contours of mutual information that a second vehicle would obtain for making a measurement from that point, using (a) the single-node approximation versus (b) the pairwise-node approximation. The brighter the contour, the more mutual information is available for sensing from that location. Using the single-node approximation, the second vehicle would tend to move along side the first vehicle. Using the pairwise-node approximation, the second vehicle would prefer to fan out. The arrows indicate the preferable directions of travel from potential current positions of the second vehicle. The scenario shown is a rescue beacon search, following actions from $t = 2$.

the probability distribution of the search target's state. The techniques presented in this paper exploit the structure of these probability distributions of the target state and the sensor measurements to find control inputs leading to future observations that minimize the expected future uncertainty of the target state. Formulae were derived to compute information-theoretic quantities using particle filters, and single-node and pairwise-node approximations were derived to enable scalability in network size. Analytical bounds were found for the error incurred by the approximations, and the pairwise-node approximation was proven to be a more accurate objective function than the single-node approximation.

The methods were demonstrated in simulated target searches using three sensing modalities. Bearings-only sensor results provide comparison to previous work that used parametric, linearized methods. The performance is demonstrated in Monte Carlo experiments. Range-only sensor results show the ability to handle a sensing scenario that is simple to understand, yet complicated to solve using parametric methods. They illustrate the ability of the proposed algorithms to capture common nonlinear effects such as saturation. Finally, the avalanche rescue beacon search results exemplify the ability of the techniques to handle problems that would pose significant hurdles to previous methods.

Several directions exist for future work, including analyzing the benefits and complications of including longer time horizons, and extending the simulations to moving targets. The algorithms are currently being implemented on STARMAC quadrotor helicopters. This experiment will demonstrate autonomous localization of a search target by a mobile sensor network using particle filter mutual information methods. The algorithms have been run in real-time on STARMAC flight computers. The techniques presented in this paper open the door to a variety of future applications. They provide methods to decouple information, and to directly use particle filters to quantify and actively seek available information.

References

[1] P. S. Maybeck, *Stochastic Models, Estimation, and Control*. New York: Academic Press, 1982, vol. 141–3.

[2] N. Gordon, D. Salmond, and A. Smith, "Novel approach to nonlinear/non-gaussian bayesian state estimation," *Proc. Inst. Elect. Eng. F*, vol. 140, no. 2, pp. 107–113, Apr. 1993.

[3] W. W. Cochran and R. D. Lord Jr., "A radio-tracking system for wild animals," *J. Wildlife Manag.*, vol. 27, no. 1, pp. 9–24, Jan. 1963.

[4] J. Hightower and G. Borriello, "Location systems for ubiquitous computing," *IEEE Computer*, vol. 34, no. 8, pp. 57–66, Aug. 2001.

[5] J. Schweizer and G. Krüsi, "Avalanche rescue beacon testing," in *Proc. Int. Snow Science Workshop*, Penticton, BC, Canada, Oct. 2002, [CD ROM].

[6] G. M. Hoffmann, H. Huang, S. L. Waslander, and C. J. Tomlin, "Quadrotor helicopter flight dynamics and control: Theory and experiment," in *Proc. AIAA Guid., Navig., Control Conf.*, Hilton Head, SC, Aug. 2007, [CD ROM].

[7] A. A. Feldbaum, "Dual control theory I-IV," *Autom. Remote Control*, vol. 21, pp. 874–880, 1960.

[8] K. B. Ariyur and M. Krstić, *Real-Time Optimization by Extremum-Seeking Control*. Hoboken, NJ: Wiley, 2003.

[9] B. Grocholsky, A. Makarenko, and H. Durrant-Whyte, "Information-theoretic coordinated control of multiple sensor platforms," in *Proc. IEEE Int. Conf. Robot. Autom.*, Taipei, Taiwan, Sep. 2003, pp. 1521–1526.

[10] T. H. Chung, V. Gupta, J. W. Burdick, and R. M. Murray, "On a decentralized active sensing strategy using mobile sensor platforms in a network," in *Proc. 43rd IEEE Conf. Decision Control*, Dec. 2004, pp. 1914–1919.

[11] E. Frew, "Observer Trajectory Generation for Target-Motion Estimation Using Monocular Vision," Ph.D. dissertation, Dept. Aero. Astro., Stanford Univ., Stanford, CA, 2003.

[12] S. Martínez and F. Bullo, "Optimal sensor placement and motion coordination for target tracking," *Automatica*, vol. 42, no. 4, pp. 661–668, 2006.

[13] J. Kim and S. Rock, "Stochastic feedback controller design considering the dual effect," in *Proc. AIAA Guid., Navig., Control Conf.*, Keystone, CO, Aug. 2006, [CD ROM].

[14] S. Thrun, W. Burgard, and D. Fox, *Probabilistic Robotics*. Cambridge, MA: MIT Press, 2005.

[15] L. Perea, J. How, L. Breger, and P. Elosegui, "Nonlinearity in sensor fusion: Divergence issues in EKF, modified truncated SOF, and UKF," in *Proc. AIAA Guid., Navig., Control Conf.*, Hilton Head, SC, Aug. 2007, [CD ROM].
[16] B. Ristic, S. Arulampalam, and N. Gordon*, Beyond the Kalman Filter: Particle Filters for Tracking Applications*. Boston, MA: Artech House, 2004.
[17] , A. Gelb, Ed.*, Applied Optimal Estimation*. Cambridge, MA: MIT Press, 1974.
[18] F. Bourgault, T. Furukawa, and H. F. Durrant-Whyte, "Decentralized bayesian negotiation for cooperative search," in *Proc. IEEE/RSJ Int. Conf. Intell. Robot. Syst.*, Sendai, Japan, Sep. 2004, pp. 2681–2686.
[19] F. Zhao, J. Shin, and J. Reich, "Information-driven dynamic sensor collaboration," *IEEE Signal Processing Mag.*, pp. 61–72, Mar. 2002.
[20] N. E. Leonard, D. A. Paley, F. Lekien, R. Sepulchre, D. M. Fratantoni, and R. E. David, "Collective motion, sensor networks, and ocean sampling," *Proc. IEEE*, vol. 95, no. 1, pp. 48–74, Jan. 2007.
[21] X. Feng, K. A. Loparo, and Y. Fang, "Optimal state estimation for stochastic systems: An information theoretic approach," *IEEE Trans. Autom. Control*, vol. 42, no. 6, pp. 771–785, Jun. 1997.
[22] C. Kreucher, K. Kastella, and A. O. Hero, III, "Information based sensor management for multitarget tracking," in *Proc. SPIE*, Bellingham, WA, Aug. 2003, vol. 5204, pp. 480–489.
[23] J. Tisdale, A. Ryan, Z. Kim, D. Törnqvist, and J. K. Hedrik, "A multiple uav system for vision-based search and localization," in *Proc. AACC Amer. Control Conf.*, Seattle, WA, 2008, pp. 1985–1990.
[24] A. Ryan, "Information-theoretic tracking control based on particle filter estimate," in *Proc. AIAA Guid., Navig., Control Conf.*, Honolulu, HI, Aug. 2008, [CD ROM].
[25] J. L. Williams, "Information Theoretic Sensor Management," Ph.D. dissertation, Mass. Inst. Tech., Elect. Eng., Cambridge, MA, 2007.
[26] G. M. Hoffmann, S. L. Waslander, and C. J. Tomlin, "Mutual information methods with particle filters for mobile sensor network control," in *Proc. 45th IEEE Conf. Decision Control*, San Diego, CA, Dec. 2006, pp. 1019–1024.
[27] F. Gustafsson, F. Gunnarsson, N. Bergman, U. Forssell, J. Jansson, R. Karlsson, and P.-J. Nordlund, "Particle filters for positioning, navigation and tracking," *IEEE Trans. Signal Processing*, vol. 50, no. 2, pp. 425–437, Feb. 2002.
[28] C. E. Shannon, "A mathematical theory of communication," *Bell Syst. Tech. J.*, vol. 27, pp. 379–423, Oct. 1948.
[29] T. M. Cover and J. A. Thomas*, Elements of Information Theory*. New York: Wiley, 1991.
[30] , A. Doucet, N. de Freitas, and N. Gordon, Eds.*, Sequential Monte Carlo Methods in Pracice*. New York: Springer, 2001.
[31] D. Crisan and A. Doucet, "A survey of convergence results on particle filtering methods for practitioners," *IEEE Trans. Signal Processing*, vol. 50, no. 3, pp. 736–746, Mar. 2002.
[32] A. Doucet, S. Godsill, and C. Andrieu, "On sequential monte carlo sampling methods for bayesian filtering," *Stat. Comput.*, vol. 10, no. 3, pp. 197–208, 2000.
[33] N. Bergman, "Recursive Bayesian Estimation: Navigation and Tracking Applications," Ph.D. dissertation, Dept. Elect. Eng., Linköpings Univ., Linköping, Sweden, 1999.
[34] P. Moin*, Fundamentals of Engineering Numerical Analysis*. New York: Cambridge Univ. Press, 2001.
[35] G. Inalhan, D. M. Stipanovic, and C. J. Tomlin, "Decentralized optimization, with application to multiple aircraft coordination," in *Proc. 41st IEEE Conf. Decision Control*, Las Vegas, NV, Dec. 2002, pp. 1147–1155.
[36] D. G. Luenberger*, Linear and Nonlinear Programming*, 2nd ed. Boston, MA: Kluwer Academic, 2003.
[37] G. Mathews, H. Durrant-Whyte, and M. Prokopenko, "Asynchronous gradient-based optimisation for team decision making," in *Proc. 46th IEEE Conf. Decision Control*, New Orleans, LA, Dec. 2007, pp. 3145–3150.
[38] J. Langelaan and S. Rock, "Navigation of small UAVs operating in forests," in *Proc. AIAA Guid., Navig., Control Conf.*, Providence, RI, Aug. 2004, pp. 468–473.
[39] D. Atkins, "Companion rescue and avalanche transceivers: The U.S. experience," *Avalanche Rev.*, vol. 17, no. 9, 1998, [CD ROM].
[40] F. Michahelles and B. Schiele, "Better rescue through sensors," in *Proc. 1st Int. Workshop Ubiquitous Comput. Cognitive Aids (UbiComp'02)*, Sep. 2002, [CD ROM].
[41] P. Piniés, J. D. Tardós, and J. Neira, "Localization of avalanche victims using robocentric slam," in *Proc. IEEE/RSJ Int. Conf. Intell. Robot. Syst.*, Beijing, China, Oct. 2006, pp. 3074–3079.
[42] J. Hereford and B. Edgerly, "457 khz electromagnetism and the future of avalanche transceivers," in *Proc. Int. Snow Sci. Workshop*, Big Sky, MT, 2000, [CD ROM].
[43] N. Ida*, Engineering Electromagnetics*, 2nd ed. New York: Springer, 2004.

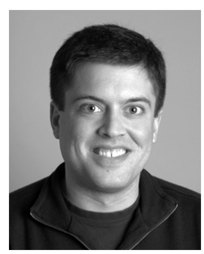

Gabriel M. Hoffmann (M'06) received the B.S. and M.S. degrees in engineering mechanics and astronautics from the University of Wisconsin-Madison, and the M.S. and Ph.D. degrees in aeronautics and astronautics from Stanford University, Stanford, CA, in 2004 and 2008, respectively.

He is a Researcher in the Intelligent Systems Lab, Palo Alto Research Center, Palo Alto, CA. He interned at Boeing and NASA Ames, flew experiments in NASA's RGSFOP, and was a Research Assistant in Stanford's Hybrid Systems Lab. His research is in autonomous vehicle control, sensor networks, and control of distributed embedded systems.

Dr. Hoffmann received the National Defense Science and Engineering Grant and was on the Stanford Racing Team that won the DARPA Grand Challenge.

Claire J. Tomlin (S'94–M'08–SM'06) is a Professor in the Department of Electrical Engineering and Computer Sciences, University of California, Berkeley, and holds a part-time Research Professor position in the Department of Aeronautics and Astronautics, Stanford University, Stanford, CA. She has held visiting researcher positions at NASA Ames and Honeywell. Her research is in the area of hybrid control systems, with applications to air traffic systems, unmanned aerial vehicles, and systems biology.

Dr. Tomlin received the MacArthur Fellowship (2006), the Okawa Foundation Research Grant (2006), and the Eckman Award from the AACC (2003).